

Automatic Multi-Stepping Approach for Ice Predictions

P.G. VERDIN and C.P. THOMPSON
Applied Mathematics and Computing Group
Cranfield University
Bedford MK43 0AL
UNITED KINGDOM
<http://www.cranfield.ac.uk/sme/amac>

Abstract: - Ice growth calculations are generally limited to a single step covering the entire icing exposure, with all relevant parameters taken as constant and calculated on the clean body. For large ice accretions, it can be necessary to recalculate the flow and icing parameters as their value vary when ice accretes. This procedure is known as multi-stepping and appears reasonable under rime and glaze ice type regimes. A manual multi-stepping ice calculation is generally possible. However, an automatic multi-stepping ice prediction is often difficult to obtain. The present paper describes the automatic multi-stepping procedure implemented in the ice prediction code ICECREMO. Results obtained on a three-dimensional airfoil are discussed and compared with experimental shapes from the literature. Limitations of the code have been identified and are being addressed within the ICECREMO2 project.

Key-Words: - Icing, ice accretion, multi-stepping, phase change, modelling

1 Introduction

The ice growth occurs when supercooled droplets impinge and freeze on the unprotected regions of an aircraft during certain flying conditions. This accretion globally affects the control, stability and aerodynamic performances of the aircraft [1-4]. Wind-tunnel measurements and in-flight tests being rather difficult and expensive, computational fluid dynamics (CFD) simulations have been developed. A great advantage of such a tool is that complex geometries may be produced and specific atmospheric conditions applied on the studied bodies.

In most cases, the ice accretion model is based on the work of Messinger [5]. However, this model has well known limitations, described in details in [6]. Physically more realist, a new type of icing codes associate full film flow analysis and the Stefan phase change [7] at the interface between the ice and water layers [8-10]. The method partially solves the difficulties created by the Messinger approach, as it is based on conduction through the layers and introduces some time dependence.

The complete icing and flow model developed by Myers et al. [8,9], is the base of the aircraft icing code ICECREMO. The ice accretion is generally limited to a single-step covering the entire icing exposure using constant values for water droplet catch, heat transfer coefficient and air shear. A

single-step approach may be accurate in rime ice type regimes, when the global ice shape does not change significantly. However, under a glaze ice type regime, it may be necessary to re-evaluate the flow and physical parameters to insure a better accuracy of the predicted ice shapes. Flow field and parameters are then re-calculated at regular time intervals. This approach, known as multi-stepping, is implemented in most of the Messinger based codes, generally for ice analysis on two-dimensional airfoils, see for instance Refs. [11-15]. Even if a manual multi-stepping ice calculation is generally possible, an automatic multi-stepping ice prediction is often difficult to obtain. This paper describes the first attempt to implement an automatic multi-stepping procedure in a Stefan based code for an ice analysis on three-dimensional airfoils.

2 General Description

Despite his small thickness, the ice layer modifies the flow around the airfoil significantly. Key parameters like the catch, the convective heat transfer coefficient or the shear stress, will be affected. These parameters, together with the external flow are then periodically recalculated. This is achieved using a time-stepping approach: the icing exposure time is divided into a specific number of time-steps, defined by the user.

Fig.1 shows a simplified algorithm of the ice accretion calculation using ICECREMO. A structured mesh is first generated around a substrate, imported into the flow solver. An ice prediction is then performed.

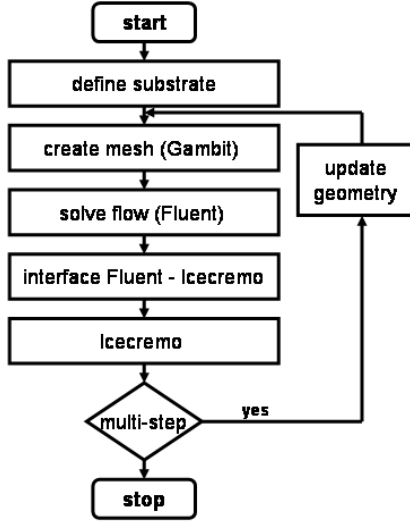


Fig1: Icing Code Algorithm

This procedure describes a one-step calculation. If a multi-step prediction is required, the substrate is updated with the ice and water layers. The process is repeated all over again, until the total ice accretion time is reached.

3 Geometry Generation

The tests presented here, have been conducted on a three-dimensional NACA0012 airfoil. The geometry and the mesh around the profile have been generated using Gambit, part of the Fluent package [16]. The structured mesh is created for each step of the multi-stepping procedure in the first instance on the clean airfoil, i.e. on the airfoil without any ice or water accretions. In the following steps, the surface is updated with the ice and water layers.

To automatically add ice in a consistent manner and to avoid crashes of the code for multiple time steps, the iced surface was enhanced prior to the next step. The simplest way to achieve it was to smooth the rough surfaces in the regions where the automatic mesh could not be obtained. The automatic generation of the solving mesh, is therefore achieved using a “journal file” which is one of the useful capabilities of the mesh generator.

4 Flow Solution

To evaluate the trajectories of the droplets, the air velocity must be known at every position the

droplets occupy. In the present analysis, the flow has been evaluated using Fluent. Trajectories and catch efficiency are calculated internally in ICECREMO using a particle tracking routine [17]. As for the mesh generation, boundaries and solving equations are automatically created via journal files.

The flow past the airfoil is modelled using the balances of mass, momentum (using full compressible Navier-Stokes equations) and energy for a perfect gas. The versatile CFD solver offers several turbulence models, including the Spalart-Allmaras one-equation model [18]. This model has been preferred for the computations as it is well known to be robust for such a study [19, 20]. Fluent uses a finite volume method: fluxes at the cell faces are interpolated using a second-order upwind scheme. Furthermore, convenient boundary conditions were applied on the control volume, including the airfoil surface.

A limitation of the automatic procedure is that specific improvement of the flow solution is not possible during a multi-stepping calculation. Input files, and a fortiori input parameters, are created and established in the first step. They remain unchanged for each following step. This may lead to difficulties to obtain a converged solution when the iced substrate becomes rough or presents large irregularities.

5 Thermodynamic Model

The thermodynamic model used in the ice accretion predictions is briefly presented in this part. However, a complete description may be obtained in Refs. [8,9,21]. In the predictions, the thicknesses of the ice and water layers are considered, denoted b and h respectively. The water layer moves mainly under the influence of gravity and air shear. It is assumed that the water layer is present as a thin film, with a lubrication theory approach being used to derive an expression for the film height. An energy balance is performed at the interface between both layers, see Fig.2. The latent heat released when water freezes, is conducted through the ice and water layers. This leads to the Stefan condition:

$$\rho_i L_f \frac{\partial b}{\partial t} = \kappa_i \frac{\partial T}{\partial z} - \kappa_w \frac{\partial \theta}{\partial z}, \quad (1)$$

where the coefficients ρ_i , L_f , b , κ_i , κ_w , T and θ are the density in the ice, the latent heat of fusion, the thickness of the ice layer, the thermal

conductivity in the ice and water layers, the temperatures in the ice and water layers, respectively.

The ice accretion rate $\partial b / \partial t$ has to be evaluated. It can be determined by considering the thermal problem, governed by heat equations in the ice and water layers [9]:

$$\frac{\partial T}{\partial t} = \frac{\kappa_i}{\rho_i c_i} \frac{\partial^2 T}{\partial z^2}, \quad (2)$$

$$\frac{\partial \theta}{\partial t} = \frac{\kappa_w}{\rho_w c_w} \frac{\partial^2 \theta}{\partial z^2}, \quad (3)$$

with C_i and C_w the specific heats capacities of the ice and water layers respectively. Considering that the temperatures in both ice and water layers do not vary significantly with time,

$$\frac{\partial T}{\partial t} \approx \frac{\partial \theta}{\partial t} \approx 0. \quad (4)$$

The ice accretion rate is then evaluated by solving equations (2) and (3). Two cases have to be studied: the rime ice growth and the glaze ice growth.

• Rime ice

In the case of rime ice growth, the latent heat is proportional to the impinging water since all the water will freeze. The temperature profile in the ice layer may be calculated with the two boundary conditions:

$$T|_{z=b} = T_s, \quad (5)$$

$$\kappa_i \frac{\partial T}{\partial z} \Big|_{z=b} = Q_l + Q_{k,w} + Q_{k,a} - Q_d - Q_c - Q_r - Q_{sb}. \quad (6)$$

The terms on the right hand side of Eq.(6) represent the latent heat Q_l , the droplets kinetic energy $Q_{k,w}$, the aerodynamic heating $Q_{k,a}$, the cooling from incoming droplets Q_d , the convective heat transfer Q_c , the radiative heat flux Q_r and the sublimation heat flux Q_{sb} .

• Glaze ice

In this case, the latent heat is evaluated at the ice-water interface. When the temperature at the surface

reaches the fusion temperature T_f , water will start appearing. The temperature profiles in the ice and water layers may be solved with the following boundary conditions given by Eqs. (7), (8), (9) and (10):

$$\kappa_w \frac{\partial T}{\partial z} \Big|_{z=b+h} = Q_{k,w} + Q_{k,a} - Q_d - Q_c - Q_r - Q_e. \quad (7)$$

The sublimation heat flux Q_{sb} which was present in the rime ice case is now replaced by the evaporation heat flux Q_e in glaze ice conditions. Furthermore, no latent heat is present at the air-water interface since this flux is produced at the ice-water interface.

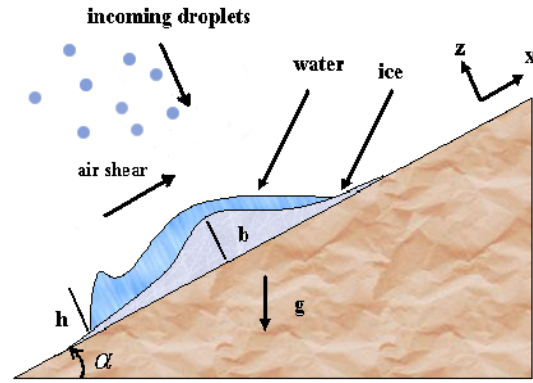


Fig.2 Problem configuration

The other boundary conditions on the surface ($z=0$) and at the ice-water interface ($z=b$) are the followings:

$$T|_{z=0} = T_s, \quad (8)$$

$$T|_{z=b} = T_f, \quad (9)$$

$$\theta|_{z=b} = T_f. \quad (10)$$

The water movement has to be studied: a mass balance may be written between the ice and water layers and the amount of incoming and remaining fluid [9]:

$$\rho_i \frac{\partial b}{\partial t} + \rho_w \left(\frac{\partial h}{\partial t} + \frac{\partial Q}{\partial x} \right) = \rho_a \beta V_a. \quad (11)$$

The ice and water growth rates $\partial b / \partial t$ and $\partial h / \partial t$ vary with the amount of impinging water $\rho_a \beta V_a$ and the movement of water on the surface described by the flux variation $\partial Q / \partial x$. This water flux takes

into account the effect of air shear, gravity and surface tension. The mass balance coupled with the energy balance provides a complete model for the icing problem.

6 Results and Discussion

The automatic multi-stepping procedure recently implemented in ICECREMO was validated in three dimensions using the airflow and icing conditions Shin and Bond used to obtain experimental ice shapes on a NACA0012 airfoil [22]. The pictures of the measured ice shapes [22] and the predicted ones from Fortin et al [23], LEWICE [24] and CIRA [25] have been extracted from Ref.[23] and added in the present paper for comparison.

Table 1 lists the airflow conditions used for the validation: airstream velocity, angle of attack, droplets diameter and air pressure. The total icing exposure was taken equal to $t_{exp} = 6min$.

V (m/s)	AoA (°)	MVD (μm)	Pa (Pa)
67.05	4	20	101300

Table 1 Airflow Conditions

Three tests are presented in this paper, under rime and glaze ice type conditions with a liquid water content equal to $LWC = 1 g/m^3$ and an airfoil chord equal to $c = 0.5334m$.

Fig.3 shows the final accumulation for both single and multi-stepping ice growth predictions performed for an ambient temperature $T_a = -5.6^\circ C$.

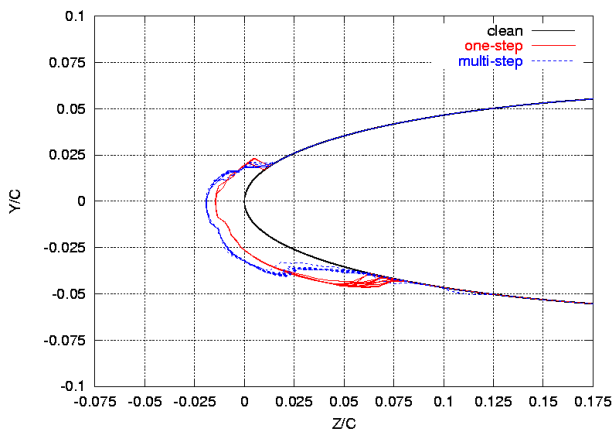


Fig.3 $T_a = -5.6^\circ C$, Single / MS Calc. (6 min) ICECREMO

Three time-steps of 2 min each have been taken for the multi-stepping prediction, while a single step of 6 min has been used in the single-step prediction. As

mentioned before, ice shapes from Fortin et al. have been extracted from Ref.[23] and added in this paper, for comparison under the same airflow and icing conditions, see Fig.4. Single and multi-stepping predictions produce almost the same ice quantity on the upper part of the airfoil, as shown in Fig.3. However, less ice is present on the lower part for multi-stepping calculations. This phenomenon may be explained by the smoothing of the surface effectuated before each re-meshing. Furthermore, the multi-stepping evaluation produces more ice in the region located near the stagnation line, where a small hollow is observed. The irregularities in the plot of the single and multi-stepping calculation are explained by the 3-D nature of the ice: the ice growth is different along the span of the wing. Furthermore, numerical errors may also lead to these irregularities observed in the multi-stepping predictions.

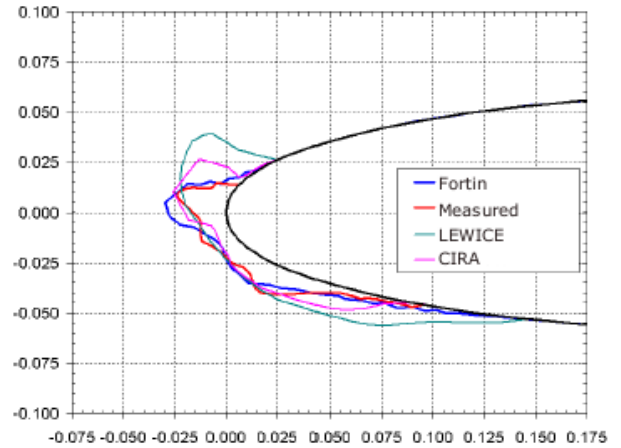


Fig.4 Ice Shapes Comparison, taken from Ref. [23] $T_a = -5.6^\circ C$ (6 min)

The resulting ice shapes obtained with ICECREMO (Fig.3) are relatively similar to the one measured experimentally, as shown in Fig.4. The predicted ice shape obtained with a 3-step evaluation seems to be more accurate than the one obtained with a single-step calculation, except in the lower part of the airfoil. For the multi-stepping prediction with ICECREMO (Fig.3), more ice is noticeable near the stagnation line and less in the upper and lower parts of the airfoil, when compared to the experimental shape (Fig.4). In a glaze ice type regime, the ice surface is smooth near the stagnation line and rough away from it. Beads appear at the transition between smooth and rough surfaces, which are difficult to predict with accuracy.

Fig.5 shows the resulting shapes for single and multi-stepping ice accretion predictions at an air temperature $T_a = -11.1^\circ C$. More ice appears on the

upper and lower parts of the surface for a single-step calculation, but less in the region close to the stagnation line. The orientation of the main ice accretion seems to have been well predicted for both single and multi-stepping calculations. A single horn shaped structure growing in the flow direction is predicted, result indicative of a rime ice type structure. The comparison between predicted and measured ice shapes shows a correct accuracy of the ice growth shapes, see Fig.5 and Fig.6. However, a small hollow may be noticed in the lower part of the airfoil for the multi-stepping calculation. In this case, it could be necessary to improve the automatic re-meshing after each time-step.

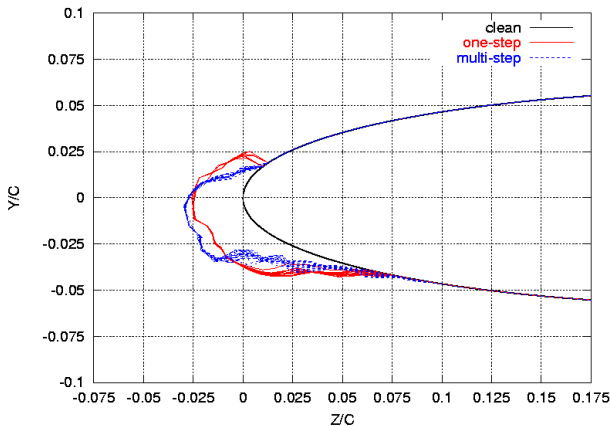


Fig.5 $T_a = -11.1^\circ\text{C}$, Single / MS Calc. (6 min) ICECREMO

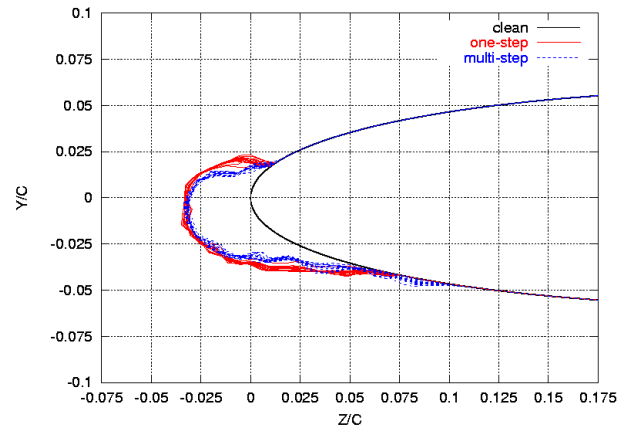


Fig.7 $T_a = -26.11^\circ\text{C}$, Single / MS Calc. (6 min) ICECREMO

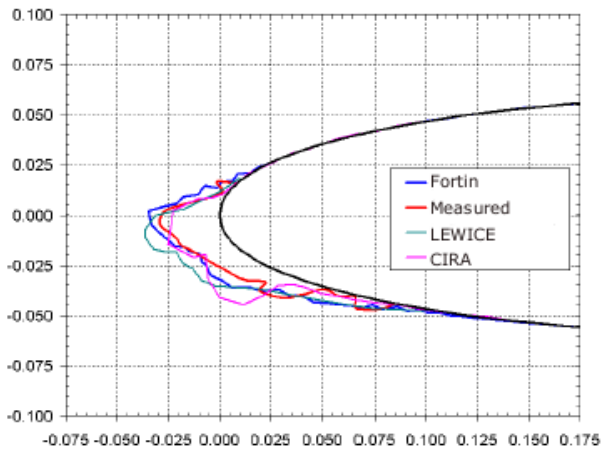


Fig.6 Ice Shapes Comparison, taken from Ref. [23] $T_a = -11.1^\circ\text{C}$ (6 min)

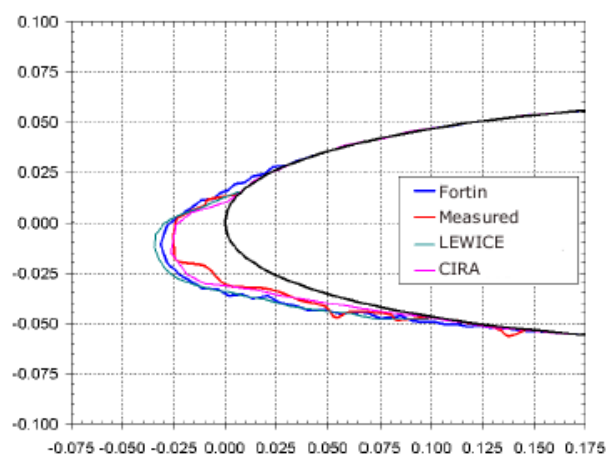


Fig.8 Ice Shapes Comparison, taken from Ref. [23] $T_a = -26.11^\circ\text{C}$ (6 min)

Fig.7 shows the resulting shapes for single and multi-stepping ice accretion predictions for an ambient temperature $T_a = -26.11^\circ\text{C}$ under a total icing exposure of $t_{exp} = 6\text{ min}$. A 2-step calculation of 3 min each has been conducted under the icing conditions listed in Table 1. No significant changes in the ice shape may be observed between both predictions. Only a small difference is noticeable

between single and multi-step predictions on the upper and lower parts of the airfoil. Once again, this is due to the procedure adopted to smooth the iced surface between each time-step. The resulting shape obtained with ICECREMO (Fig.7), is typical of the ones obtained in rime ice conditions and is similar to those measured experimentally, as shown in Fig.8. Nevertheless, the quantity of ice found is slightly bigger in the airflow direction for single and multi-stepping calculations than for the measured one. In the region close to the lower part of the airfoil, the predicted shapes are slightly smaller than the experimental shapes.

7 Conclusion

A description of the first implementation of an automatic multi-stepping procedure in a Stefan-based code has been briefly presented in this paper. Although further developments are necessary to improve the automatic predictions, the results obtained with ICECREMO are very encouraging.

Multi-stepping calculations should largely improve the accuracy of the predicted ice shapes. However, the actual limitations of the code (only a structured mesh is accepted and the thermal history within the ice is not preserved from one step to the next), lead to difficulties to obtain correct final shapes. They will be addressed in the improved version of the code (ICECREMO2), currently developed in UK. An automatic multi-stepping procedure will also be implemented in the new unstructured version. Final ice shapes are expected to be predicted with a higher accuracy.

Acknowledgment:

This work was sponsored by Westland Helicopters Ltd, under the ICECREMO2 contract, which is jointly funded by the Department of Trade and Industry (UK), Airbus UK, BAe Systems, Dunlop Aerospace, QinetiQ (formerly the Defense Evaluation and Research Agency, DERA), Rolls-Royce and Westland Helicopters Ltd. Cranfield University acts as the main sub-contractor.

References:

- [1] S. Thomas, R. Cassoni and C. MacArthur, Aircraft anti-Icing and deicing techniques and modeling, *AIAA Paper 96-0390*, 1996.
- [2] M.G. Potapczuk and B.M Berkowitz, Experimental investigation of multi-element airfoil ice accretion and resulting performance degradation, *NASA TM-101441*, Jan. 1989.
- [3] S. Lee and M.B. Bragg, Experimental investigation of simulated large-droplet ice shapes on airfoil aerodynamics, *Journal of Aircraft*, Vol.36, 1999, pp. 844-850.
- [4] R.W. Gent, N.P. Dart and J.T. Cansdale, Aircraft icing, *Phil. Trans. R. Soc. Lond.*, A358, 2000, pp. 2873-2911.
- [5] B.L. Messinger, Equilibrium temperature of an unheated icing surface as function of airspeed, *J. Aeronaut. Sci.*, Vol.20, No.1, 1953, pp. 29-42.
- [6] T.G. Myers, An extension to the Messinger model for aircraft icing, *AIAA Journal*, Vol.39 (2), 2001, pp. 211-218.
- [7] B. Sarler, Stefan's work on solid-liquid phase changes, *Engineering Analysis with Boundary Elements*, Vol.16 (2), 1995, pp. 83-92.
- [8] T.G. Myers and D. Hammond, Ice and water film growth from incoming supercooled droplets, *International Journal of Heat and Mass Transfer*, Vol.42, 1999, pp. 2233-2242.
- [9] T.G. Myers, J.P.F. Charpin and C.P. Thompson, Slowly accretion ice due to supercooled water impacting on a cold surface, *Physics of Fluids*, Vol.14, No.1, 2002, pp. 240-256.
- [10] T.G. Myers, J.P.F. Charpin and S.J. Chapman, The flow and solidification of a thin fluid film on an arbitrary three-dimensional surface, *Physics of Fluids*, Vol.14, No.8, 2002, pp. 2788-2803.
- [11] G.A. Ruff and B.M. Berkowitz, Users manual for the NASA Lewis ice accretion prediction code (LEWICE), *TR CR-185129*, May 1990.
- [12] S. Eberhardt and H. Ok, Aircraft icing predictions using an efficient incompressible Navier-Stokes solver, <http://www.aa.washington.edu/faculty/eberhardt/icing.pdf>
- [13] R.W. Gent, TRAJICE2 - A combined water droplets trajectory and ice accretion prediction program for aerofoils, *Technical Report TR-90054*, Royal Aircraft Establishment, UK, 1990.
- [14] T. Hedde and D. Guffond, Development of a three-dimensional icing code, comparison with experimental shapes, *AIAA Paper 92-0041*, 1992.
- [15] G. Mingione and V. Brandi, Ice accretion prediction on multi-elements airfoils, *Journal of Aircraft*, Vol.35, No.2, 1998, pp. 240-246
- [16] <http://www.fluent.com>
- [17] A.J. Press and N.P. Dart, ICECREMO User Guide, *ICECREMO/SPEC/DERA/ND990506/3*, March 2000.
- [18] P.R. Spalart and S.R. Allmaras, A one-equation turbulence model for aerodynamic flows, *AIAA paper 92-0439*, 1992.
- [19] J.J. Chung and H.E. Addy, A numerical evaluation of icing effects on a natural laminar flow airfoil, *AIAA Paper 2000-0096*, 2000.
- [20] X. Chi, B. Zhu, T.I-P. Shih, H.E. Addy and Y.K. Choo, CFD analysis of the aerodynamics of a business-jet airfoil with leading-edge ice accretion, *AIAA Paper 2004-0560*, 2004.
- [21] J.P.F. Charpin, *Water flow on accreting ice surfaces*, PhD Thesis, School of Engineering, Cranfield University, UK, Sept. 2002.
- [22] J. Shin and T.H. Bond, Results of an icing test on a NACA 0012 Airfoil in the NASA Lewis Icing Research Tunnel, *AIAA Paper 92-0647*, 1992.
- [23] G. Fortin, J.L. Laforte and A. Beisswenger, Prediction of ice shapes on NACA0012 2D airfoil, *SAE Technical Papers 2003-01-2154*, 2003.
- [24] J. Shin and T.H. Bond. Experimental and Computational Ice Shapes and Resulting Drag Increase for a NACA0012 Airfoil, *NASA TM 105743*, 1992.
- [25] G. Mingione, V. Brandi and B. Esposito, Ice accretion prediction on multi-element airfoil, *AIAA Paper 97-0177*, 1997.